

Temperature dependent optical studies of $\text{Ti}_{1-x}\text{Co}_x\text{O}_2$

S. Guha,^{1,*} K. Ghosh,¹ J.G. Keeth,¹ S. B. Ogale,² S.R. Shinde,² J. R. Simpson,³ H. D. Drew,³ and T. Venkatesan³

¹*Department of Physics, Astronomy and Materials Science, Southwest Missouri State University, Springfield, MO 65804 USA*

²*Center for Superconductivity Research, Department of Physics, University of Maryland, College Park, MD 20742-4111*

³*Department of Physics, University of Maryland, College Park, MD 20742-4111*

(Dated: November 3, 2018)

Abstract

We present the results of Raman and photoluminescence (PL) studies on epitaxial anatase phase $\text{Ti}_{1-x}\text{Co}_x\text{O}_2$ films for $x = 0-0.07$, grown by pulsed laser deposition. The low doped system ($x=0.01$ and 0.02) shows a Curie temperature of 700 K in the as-grown state. The Raman spectra from the doped and undoped films confirm their anatase phase. The photoluminescence spectrum is characterized by a broad emission from self-trapped excitons (STE) at 2.3 eV at temperatures below 120 K. This peak is characteristic of the anatase-phase TiO_2 and shows a small blueshift with increasing doping concentration. In addition to the emission from STE, the Co-doped samples show two emission lines at 2.77 eV and 2.94 eV that are absent in the undoped film indicative of a spin-flip energy.

Dilute magnetic semiconductors (DMS) based on II-VI semiconductors, such as Mn-doped CdTe and ZnSe,¹ and III-Vs, such as Mn-doped GaAs² have been studied extensively in the last decade due to their potential usage of both charge and spin degrees of freedom of carriers in electronic devices. However, these materials undergo a ferromagnetic phase transition temperature much below room temperature. The discovery of ferromagnetism with Curie temperatures above 300 K in cobalt-doped TiO₂ has generated considerable amount of interest in this system and similar oxide based ferromagnetic semiconductors.^{3,4} First-Principles calculations of Co-doped TiO₂ elucidate on the electronic structure and microscopic distribution of Co atoms crucial for ferromagnetic ordering.^{5,6} Recently, Mn-doped GaN films are also known to show room temperature ferromagnetism.^{7,8}

TiO₂ is a wide band gap semiconductor with excellent transmittance in the visible and near-infrared regions, high refractive index, and high dielectric constant. It occurs in three crystal structures: rutile, anatase, and brookite. Anatase TiO₂ is composed of stacked edge-sharing octahedrons formed by six oxygen anions. There are significant differences in the electronic structure between the anatase and rutile crystal structures. Anatase TiO₂ has a very shallow donor level and high electron mobilities compared to the rutile phase.⁹ The *n*-type carriers in TiO₂ result from oxygen vacancies, which provide tunability to its properties. Detailed investigations of the absorption edges in anatase and rutile phases by Tang *et al.* have shown that that the excitonic states of the anatase phase are self-trapped while that of the rutile phase are free.¹⁰

In this work we present the results of Raman and photoluminescence (PL) studies on epitaxial anatase phase Ti_{1-x}Co_xO₂ films for $x = 0, 0.01, 0.02, 0.04,$ and $0.07,$ grown by pulsed laser deposition (PLD). Thin films of Ti_{1-x}Co_xO₂ were deposited at a pressure of $2-4 \times 10^{-5}$ on LaAlO₃ (001) substrates by PLD, using sintered targets synthesized by the standard solid-state route. The substrate temperature, laser energy, and pulse repetition rate were kept at 700 °C, 1.8 J/cm², and 10 Hz, respectively. The thickness of the films were ≈ 100 nm.

X-ray diffraction (XRD) was employed for structural characterization. The hysteresis loops and magnetization were obtained using a SQUID magnetometer. The Raman measurements were carried out in a backscattering geometry using a fiber-optically coupled confocal micro-Raman system (TRIAx 320) equipped with a liquid N₂ cooled charge coupled detector. The 514.5 nm line of an Ar⁺ ion laser was the excitation source. The microscope is

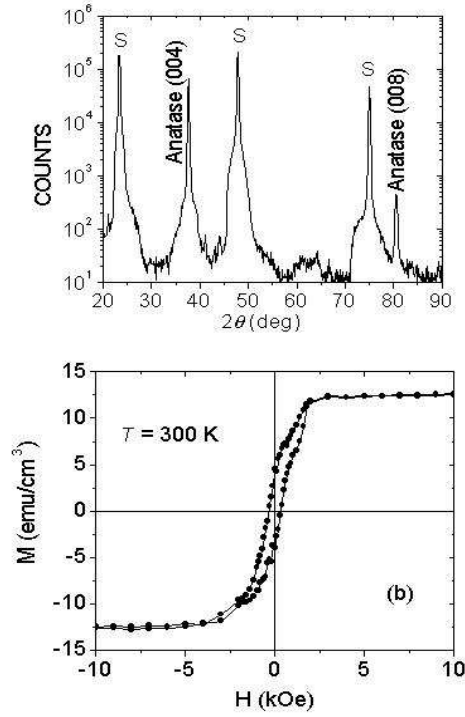


FIG. 1: (a) XRD pattern and (b) 300 K hysteresis loop of $\text{Ti}_{0.98}\text{Co}_{0.02}\text{O}_2$. In (a) the substrate peaks are labelled by "s".

equipped with a holographic super-notch filter to block the elastically scattered light. A 50 X microscope objective was used to focus and collect the scattered laser light, with a spatial resolution of about $5\mu\text{m}$. The PL spectra were excited using the 363.8 nm line of an Ar^+ laser. The luminescence excitation was analyzed with a SPEX 0.85 m double monochromator equipped with a cooled GaAs photomultiplier tube and standard photon counting electronics. For low temperature measurements a closed cycle refrigerator was employed.

Figure 1 (a) and (b) shows the XRD pattern and the magnetic response, respectively, of $\text{Ti}_{0.98}\text{Co}_{0.02}\text{O}_2$ on LaAlO_3 (001). The (004) and the (008) peaks of the anatase phase are clearly observed in the XRD. The XRD rocking curve full width at half maximum of the sample peaks are $\sim 0.3^\circ$. The magnetic response was measured as a function of the magnetic field strength at room temperature. Hysteresis is observed indicating that the film is ferromagnetic even at room temperature. The low doped system ($x=0.01$ and 0.02) shows a Curie temperature of ~ 700 K in the as-grown state.⁴ The anatase and the rutile phase belong to the symmetry space groups D_{4h}^{19} and D_{4h}^{14} , respectively.¹¹ Group theory predicts six Raman active modes for the anatase phase; E_g : 147 cm^{-1} , E_g : 198 cm^{-1} , B_{1g} : 398 cm^{-1} , A_{1g} and B_{1g} : 515 cm^{-1} , and E_g : 640 cm^{-1} . The rutile phase has four Raman active modes, the predominant ones are E_g : 448 cm^{-1} , A_{1g} : 612 cm^{-1} , and B_{1g} : 827 cm^{-1} . Since the

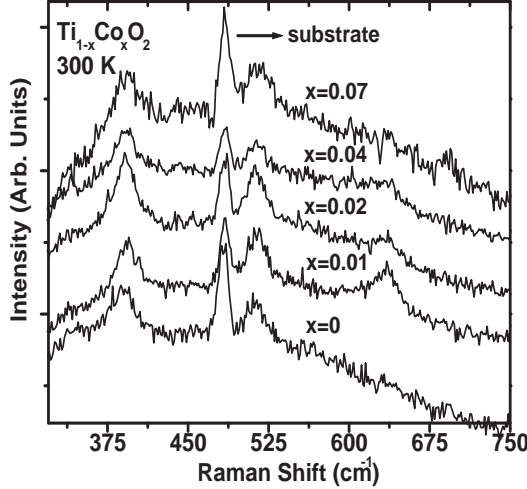


FIG. 2: Raman spectra of $\text{Ti}_{1-x}\text{Co}_x\text{O}_2$ for values of x at 300 K. The peak at 485 cm^{-1} is from the substrate.

Raman peaks from each phase are clearly separated in frequency, the two phases are easily distinguishable by their Raman spectra.

Figure 2 shows the Raman spectra from $\text{Ti}_{1-x}\text{Co}_x\text{O}_2$ for various Co concentrations. The 485 cm^{-1} peak is from the LaAlO_3 substrate and serves as a good calibrant. Since the notch filter cuts off energy positions below 200 cm^{-1} , we do not observe the low energy E_g Raman peaks. The Raman peaks at 398 cm^{-1} and 515 cm^{-1} clearly show that the samples are in the anatase phase. A signature of the 640 cm^{-1} is observed for $x=0.01$ and 0.02 samples. Within the experimental accuracy of a few wavenumbers there is no discernable shift of the Raman peaks of the sample with higher Co-doping concentration. However, for the higher Co-doped samples the Raman peaks broaden. This may be an indication of limited Co solubility resulting in a disorder of the crystal structure. A recent work by Shinde *et al.* shows that higher Co-doping (beyond $x=0.02$) without annealing results in the formation of Co clusters in $\text{Ti}_{1-x}\text{Co}_x\text{O}_2$.⁴

Though the absorption edge of anatase TiO_2 is at $\sim 3.2\text{ eV}$, the luminescence spectrum Stokes shifts by almost 1 eV . A broad greenish-yellow emission, centered at 2.3 eV is observed from films and crystals of anatase TiO_2 .^{10,12} The TiO_6 octahedra in the anatase phase are distorted to lower symmetry, which lifts degeneracies and creates band splitting resulting in a narrowing of the conduction band. The band-to-band excitation therefore results in self-trapped excitonic states due to a localization of the excited state and its energy is lowered by the lattice relaxation energy.¹⁰

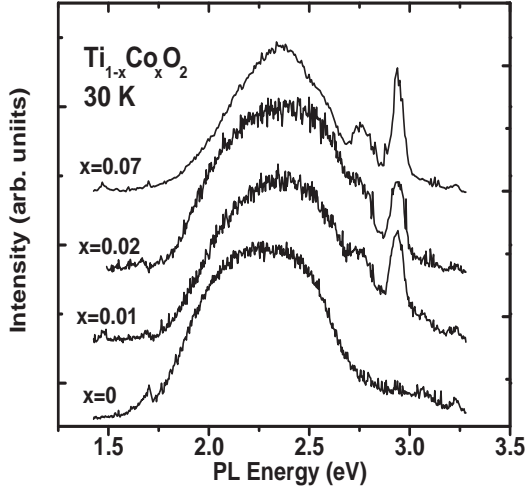


FIG. 3: PL spectra of $\text{Ti}_{1-x}\text{Co}_x\text{O}_2$ for various Co concentration at 30 K.

Figure 3 shows the PL spectra of $\text{Ti}_{1-x}\text{Co}_x\text{O}_2$ for various values of x , measured at 30 K. The spectra are characterized by a broad emission centered at 2.3 eV due to the self-trapped excitons. The individual spectra have been normalized to the 2.3 eV emission and vertically shifted for clarity. A recent work using polarized PL shows that this broad emission can be further resolved into at least two peaks centered at 2.2 eV and 2.4 eV.¹² The center of the self-trapped emission (STE) shows a slight blueshift in energy with increased doping concentration.

The most striking feature of Fig. 3 is the appearance of two peaks at 2.77 eV and 2.94 eV in the Co-doped samples which are absent in the undoped samples. At 30 K the 2.77 eV peak appears as a weak shoulder in the low doped samples. To understand the origin of the above peaks, we have carried out a thorough temperature dependence of the PL. Since higher cobalt doping leads to clustering in as-grown films,⁴ we compare the PL from undoped TiO_2 to the low Co-doped samples as a function of temperature.

Figure 4 shows the PL spectra for a few selected values of temperature for (a) $x=0.02$ and (b) $x=0.0$ samples. The spectra have been normalized to the STE emission for both (a) and (b). With increasing temperature the intensity of the STE drops and beyond 120 K it is barely visible. For the $x=0.02$ sample the energy position of STE shows almost no shift with increasing temperatures. This is in contrast to other doped system, such as Al-doped anatase TiO_2 , where the STE redshifts by more than 500 meV from 5 K to 150 K due to trapping of excitons at higher temperatures by Al acceptor levels.¹⁰ Our results clearly show that the cobalt impurities do not result in any additional self-trapping mechanism.

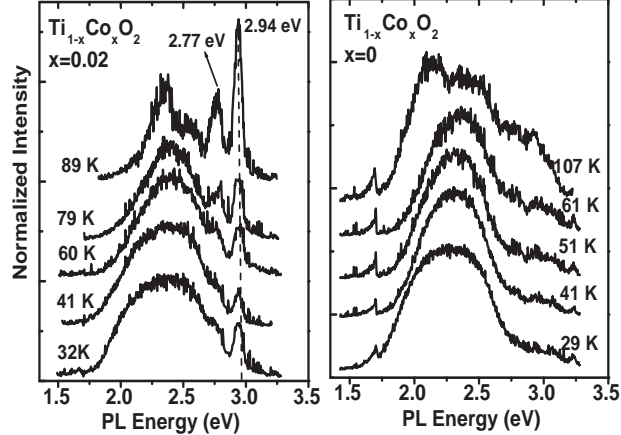


FIG. 4: PL spectra of (a) $\text{Ti}_{0.98}\text{Co}_{0.02}\text{O}_2$ and (b) undoped TiO_2 at selected values of temperature.

The absolute intensities of the 2.77 eV and 2.94 eV PL peaks do not change significantly with temperature. Since the PL spectra are normalized to the STE peak in Fig. 4 (a), it appears that the 2.94 eV and the 2.77 eV peaks gain intensity upon increasing temperatures. These two peaks are not related to any oxygen vacancies. We have compared the PL spectra (at different temperatures) from two halves of the $x=0.02$ sample: one half being the as-grown and the other half was annealed in an oxygen atmosphere. The PL spectra at all temperatures from both samples are identical, eliminating any issues related to oxygen vacancies. The difference in energy of 170 meV between the 2.77 eV and the 2.94 eV peaks may be related to states with a given spin and a spin-flipped state.

Band structure calculations show that the valence band derives primarily from oxygen p-levels, the conduction band from the Ti d-levels and the crystal-field split Co d-levels fall within the energy gap. The local-spin-density approximation (LSDA) calculations by Park *et al.* show that the crystal field splitting between t_{2g} and e_g states is larger than the exchange splitting between t_{2g} states, suggesting a low spin state of Co.⁵ The appearance of the 2.77 eV and the 2.94 eV energy levels in our PL spectra appear well below the absorption edge of 3.2 eV in $\text{Ti}_{1-x}\text{Co}_x\text{O}_2$,¹³ indicating that they most probably arise from the cobalt e_g energy levels. Moreover, the 170 meV difference between the two PL peaks agree well with the energy separation between the spin-up and spin-down e_g states of the LSDA calculation.⁵

The location of Co midgap levels also depends on the nature of the microscopic distribution of the co atoms, as seen in the work by Yang *et al.*⁶ The local oxygen non-stoichiometry (which influences the valence states of cations) also affects the band filling. Thus, the assign-

ment of the observed levels to specific electronic states would require these inputs. Based on the total energies calculated for various configurations, Yang *et al.* suggest that cobalt ions in the $\text{Ti}_{1-x}\text{Co}_x\text{O}_2$ matrix would prefer non-uniform doping mode with short Co-Co distances.⁶ Future work involving magneto-optical techniques should reveal the nature of magnetic coupling and magnetic excitations from various $\text{Ti}_{1-x}\text{Co}_x\text{O}_2$ configurations and their possible participation in optical processes.

Acknowledgments

S.G. acknowledges the donors of the American Chemical Society Petroleum Research Fund Grant No. 38193-B7 and the Research Corporation Grant No. CC5332. Work at UMD is supported under NSF-MRSEC DMR Grant No.00-80008.

* Corresponding author E-mail:sug100f@smsu.edu

- ¹ J.K. Furdyna and J. Kossut, *DMSs, Semiconductor and Semimetals* Vol.**25**, Academic Press, New York (1988).
- ² H. Ohno, A. Shen, F. Matsukura, A. Oiwa, A. Endo, S. Katsumoto, and Y. Iye, *Appl. Phys. Lett.* **69**, 363 (1996).
- ³ Y. Matsumoto, M. Murakami, T. Shono, T. Hasegawa, T. Fukumura, M. Kawasaki, P. Ahmet, T. Chikyov, S-ya Koshihara, H. Koinuma, *Science* **291**, 854 (2001).
- ⁴ S.R. Shinde, S.B. Ogale, S. Das Sarma, J. R. Simpson, H. D. Drew, S.E. Lofland, C. Lanci, J. P. Buban, N. D. Browning, V.N. Kulkarni, J. Higgins, R.P. Sharma, R.L. Greene, T. Venkatesan, (in press, *Phys. Rev. B*, 2003) arXiv:cond-mat 0203576 (2002).
- ⁵ Min Sik Park, S.K. Kwon, and B.I. Min, *Phys. Rev. B* **65**, 161201-1 (2002).
- ⁶ Z. Yang, G. Liu, and R. Wu, *Phys. Rev. B* **67**, 060402-1 (2003).
- ⁷ M.L. Reed, N.A. El-Masry, H.H. Stadelmaier, M.K. Ritums, and M.J. Reed, *Appl. Phys. Lett.* **79**, 3473 (2001).
- ⁸ T. Sasaki, S. Sonoda, K-I.Suga, S. Shimizu, K. Kindo, H. Hori, *J. Appl. Phys.* **10**,7911 (2002).
- ⁹ L. Forro, O. Chauvet, D. Emin, L. Zuppiroli, H. Berger, and F. Lévy, *J. Appl. Phys.* **75**, 633 (1994).

- ¹⁰ H. Tang, H. Berger, P.E. Schmid, F. Lévy, *Solid State Commun.* **87**, 847 (1993).
- ¹¹ M. Ocaña, J.V. Garcia-Ramos, and C.J. Serna, *J. Am. Ceram. Soc.* **75** 2010, (1992).
- ¹² V. Kiisk, I. Sildos, A. Suisalu, and J. Aarik, *Thin Solid Films* **400**, 130 (2001).
- ¹³ J.R. Simpson, H.D. Drew, S.R. Shinde, Y. Zhao, S.B. Ogale, and T. Venkatesan, submitted to *Appl. Phys. Lett.* arXiv:cond-mat cond-mat/0205626 (2002).